Mechanical and structural assessment of cortical and deep cytoskeleton reveals substrate-dependent alveolar macrophage remodeling.

Sophie Féréol, Redouane Fodil, Valérie M. Laurent, Emmanuelle Planus, Bruno Louis, Gabriel Pelle, Daniel Isabey

Mechanical and structural assessment of cortical and deep cytoskeleton reveals substrate-dependent alveolar macrophage remodeling.

S. Féréol[a], R. Fodil, V.M. Laurent[b], E. Planus[c], B. Louis, G. Pelle and D. Isabey.

Inserm UMR841, Institut Mondor de Recherche Biomédicale, Equipe Biomécanique Cellulaire et Respiratoire, Créteil, France.

Present addresses:

[a]CNRS UMR7101, Laboratoire de Neurobiologie des Signaux Intercellulaires, Régénération et Croissance Axonale, Paris, France.

[b]Université Paris V, Laboratoire de Neuro-Physique Cellulaire, Paris, France.

[c]Centre de Recherche Inserm-UJF U823, Equipe DySAD,

IAB Site Santé, La Tronche, Grenoble, France.

Correspondence address:

Daniel Isabey

Inserm UMR 841, Equipe Biomécanique Cellulaire et Respiratoire

Faculté de Médecine

8, rue du Général Sarrail

94 010 CRETEIL Cedex, France

Tél : 33 1 49 81 37 00

Fax : 33 1 48 98 17 77

E-mail : daniel.isabey@creteil.inserm.fr

Abstract:

The sensitivity of alveolar macrophages to substrate properties has been described in a recent paper (Féréol et al., *Cell Motil.Cytoskeleton*, 63: 321-340, 2006). It is presently re-analyzed in terms of F-actin structure (assessed from 3D-reconstructions in fixed cells) and mechanical properties (assessed by Magnetic Twisting Cytometry experiments in living cells) of cortical and deep cytoskeleton structures for rigid plastic (Young Modulus: 3MPa) or glass (70 MPa) substrates and a soft (~ 0.1 kPa) confluent monolayer of alveolar epithelial cells. The cortical cytoskeleton component (lowest F-actin density) is represented by the rapid and softer viscoelastic compartment while the deep cytoskeleton component (intermediate F-actin density) is represented by the slow and stiffer compartment. Stiffness of both cortical and deep cytoskeleton is significantly decreased when soft confluent monolayer of alveolar epithelial cells replace the rigid plastic substrate while F-actin reconstructions reveal a consistent actin cytoskeleton remodeling observable on both cytoskeleton components.

Introduction

In a recent review of the literature dedicated to cell sensitivity to substrate stiffness, Disher et al. [6] have pointed out that tissue cells do experiment substrate of stiffness varying by several order of magnitude. For instance, values of elasticity (Young) modulus range (i) from 1.5 kPa to 5 kPa in brain [14], (ii) from 5 kPa to 15 kPa in muscles [12] with a mean at 12 kPa [8] and (iii) from 40 to 160 kPa in skin [16], while disease conditions could result in some rigidification process [14,25]. Importantly, cells are thought to be able to provide a biological response adapted to the large diversity in surrounding tissues stiffness [6,8]. Cellular adaptation to, for instance, a stiffer mechanical environment, occurs through changes in cell shape secondary to cytoskeleton remodeling, (e.g., flattening process mostly associated to generation of stress fibers in the basal cell plane) [26,37], adjustment of cellular properties (e.g., increase in internal tension) [15], and finally modulation of major cell functions, (e.g., less migration, less proliferation…) [23,31].

Surprisingly, the cell sensitivity to tissue mechanical properties requires not only the outside-in signaling classically used to understand the cell response to external forces, but a more complex feedback loop of inside-outside-in signaling that definitely involves elasticity of the extracellular environment [6]. To mediate the cell response, the mechano-chemical signaling pathways still need to be identified. They firstly implicate the variety of adhesion sites (e.g., from the stable focal adhesion sites to the dynamic nascent adhesion sites) which all constitute physical links between intracellular to extracellular mediums and have been thought to play the role of mechanosensors [1,2,17]. Second, mechanotransduction pathways include the various types of cytoskeleton biopolymers (e.g., actin filaments, microtubules, intermediate filaments) [11,33]. For instance, the contractile forces generated by cross-bridging interactions between actin and myosin filaments are transmitted to the adhesion sites along stress fibers and thereby contribute to the inside-out signaling [1].

However complete understanding of how cells not only adhere but also sense their microenvironment and thereby respond in a way related to extracellular matrix elasticity remain to be achieved. Recently, we have explored the sensitivity to substrate stiffness of fast moving adherent cells, i.e., alveolar macrophages (AMs), which functionally differ from tissue cells [9]. The results obtained in AMs in terms of mechanosensitive pathways suggest that the highly tensed cytoskeletal elements are most likely not exclusive pathways for mechanotransduction, while tensed actin fibers were thought to contribute to transmission of mechanical signal within tensed tissue cells [2]. Noteworthy, sensitivity of AMs to substrate stiffness occurs in the absence of stress fibers and at negligible levels of internal tension [9].

The aim of the present study is to re-analyze with a deeper insight, the cytoskeleton remodeling of AMs corresponding to environmental conditions having two very different substrate stiffness, namely a glass (or plastic) substrate classically used in *in vitro* experiments and a physiologically-relevant substrate made of a confluent monolayer of alveolar epithelial cells on which AMs basically adhere and move. To do so, we have considered the associated changes in mechanical properties and in actin structure of both the cortical and deep cytoskeleton components, following a method we previously validated in cultures of alveolar epithelial cell lines (A549) [18]. Such a mechanical assessment requires a specific curve fitting analysis by two viscoelastic solid elements in series of the cellular deformation, (i.e., the mean rotation over a large population of twisted microbeads attached to macrophage cytoskeleton through integrin receptors). This cell deformation occurs in response to a step function of stress resulting from a magnetic torque created by a laboratory made Magnetic Twisting Cytometry (MTC) device previously described [20,27]. The structural rearrangement was assessed from 3D-reconstruction of the stained actin structure evidenced at two levels of fluorescent intensity in confocal images [10].

The results so re-analyzed in AM cells, show that actin structure remodeling in response to a drastic change in substrate stiffness (0.1 kPa versus 3-70 MPa) concerns both the cortical and the deep cytoskeleton. However, this structural remodeling does not resemble to that previously observed in tissue cells since it occurs without stress fibers generation even for the deep cytoskeleton structure. Consistently, the stiffness of the cortical and deep cytoskeleton is not significantly altered by cytochalasin D treatment. Importantly, the large decrease in substrate stiffness presently tested results in a significant decrease in stiffness for both the cortical and the deep cytoskeleton components. Altogether, present results suggest that the mechanical properties of cell substrate must be controlled as it could strongly influence the cellular response. Thus, cell sensitivity to mechanical environment concerns both cellular biology and cellular bioengineering studies.

Material and Methods

Culture of alveolar macrophages on epithelial monolayer or rigid substrate:

AMs were isolated from pathogen-free male or female Sprague-Dawley rats following a procedure previously described in [9]. An average yield of 4.10^6 cells/rat was obtained. After isolation of rat AMs, AMs were seeded at a density of 1.5×10^6cells/ml onto the two types of tested substrates and incubated for 3 hours on these substrates, namely the soft cellular and the rigid plastic/glass substrates. For the cellular substrate, rat type II pneumocytes were isolated as described above and then plated at a density of 10^6 cells per cm^2 on Lab-Tek® chambered coverglass (8 wells) previously coated with type I collagen. The stiffness (Young Modulus) value of the epithelial cell monolayer was taken equal to 0.1 kPa, corresponding to the typical value measured in (A549) epithelial cell monolayer by the MTC method after appropriate geometrical correction [20,24]. We have also characterized the

confluent nature of the epithelial cell monolayer by Atomic Force Microscopy (Nanowizard, JPK Instrument Berlin). Moreover, typical values of stiffness (Young Modulus) were used for the highly rigid plastic or glass surface (i.e., respectively 3 MPa and 70 MPa) [12]. These quite different substrates (i.e., epithelial cell monolayer and/or glass/plastic) aimed at mimicking the wide variety of elasticity properties of substrates encountered by the cells, e.g., between *in vitro* to *in vivo* environments. The 3 hours time allowed for AM adhesion was chosen as a compromise between optimal adhesion and minimal de-differentiation [29]. Non-adherent cells were then removed by 3 rinses with RPMI 1640 supplemented with 0.1% BSA (37°C). For each substrate studied, (i.e., cellular monolayer or glass/plastic substrate), the macrophages pertaining to the same population, (i.e., issued from the same rat) were seeded in culture wells without addition of any chemoattractant. The absence of chemo-attractant guaranteed no chemical activation of AMs in our experimental conditions, meaning that the wide majority of AMs maintained a symmetrical actin shape without front-rear polarization (see Results).

Spatial reconstruction of F-actin:

Five days later, rat type II pneumocytes had formed a confluent cell monolayer and AMs isolated by bronchoalveolar lavages were seeded over the monolayer for 3 hours before fixation and staining. The fixation of the co-culture was performed with 1% glutaraldehyde and then F-actin was stained with rhodamined phalloidin (1.5 µM), as previously described [7]. The stained F-actin cytoskeleton structure was examined with a ×100/1.3 numerical aperture Plan Neofluar objective mounted on a laser confocal microscopy (LSM 410, Zeiss, Rueil-Malmaison, France). Spatial organisation of F-actin structure was obtained from 3D-reconstructions performed from optical sections recorded every 0.3 µm which revealed intracellular fluorescence by means of a grey level scale. Contours of external and internal

subcellular structures corresponding to two different levels of fluorescent intensity where defined using the curve of the "logarithmic" decrease in cumulated pixels of the stack images versus the grey level (0 to 255). Practically, the cell image ranged from 8 to 230. The lower value detectable (i.e., 8-13) corresponded to the external boundary of the actin structure while the deep cytoskeleton structure was systematically defined at a value located at 25% of that range (i.e., ~63-67) which standardly reveals stress fibers in adherent tissue cells.

Stiffness and prestress measurements:

Cell elasticity modulus was assessed by a previously described laboratory-made Magnetic Twisting Cytometry device (MTC) [9] similar to that initially described by Wang et al. [32], i.e., based on the measure of the mean rotation over a wide population twisted ferromagnetic RGD-coated beads attached to transmembrane mechanoreceptors (integrins) linked to actin cytoskeleton. The difference with initial MTC method resides in data analysis. Indeed, the torque-bead rotation relationships used to deduce the actual cell stiffness from the apparent cell stiffness (or torque divided by the product: bead rotation×bead volume) is corrected by a factor deduced from a numerical model. The latter takes into account the half-angle of bead immersion calculated from 3D-reconstructions of the AM F-actin structure. This immersion angle was 108° ± 30° estimated for a population of 10 beads [9]. The average bead rotation angle was measured by an on-line magnetometer over the entire bead/cell population present in the culture and for a constant torque applied to the beads herein equal to 800 pN·µm (corresponding to a 5 mT perpendicular magnetic field).

AMs were plated at a density of 10^6 cells/ml in bacteriological dishes (96-well). The dishes were either or not covered by a confluent monolayer of rat pneumocytes seeded 5 days sooner after coating with type I collagen. Before use, AMs were incubated in RPMI 1640 medium supplemented with 1% BSA for at least 30 minutes at 37°C to block non-specific

binding. RGD-coated ferromagnetic beads were then added to the cells (40µg per well) for 30 minutes at 37°C in a 5% CO_2 - 95% air incubator. Unbound beads and AMs were washed away systematically three times with RPMI 1640 medium supplemented with 1% BSA. We verified in a previous study that neither the three repeated rinsing nor the torque application significantly affected the remnant magnetic field nor the stiffness measurement [24].

To study the effect of actin depolymerization on the mechanical properties of AMs plated on different substrates, we used treatments with low concentrations of cytochalasin D (cyto D) (1 µg/ml) for 11 min before MTC measurements. We have previously shown on highly structured F-actin alveolar epithelial cells (A549) adherent on glasses that the main effect of cyto D treatment primarily alters the dense F-actin network [19] resulting in a decrease in cellular prestress [35]. Hence, decay in stiffness was systematically found in adherent cells once treated with cyto D [32,34]. Subsequently, the difference in stiffness between cyto D treatment and control has been used as a quantification of prestress [27,28]. The recent findings obtained in contractile adherent cells by Wang et al. about the positive linear relationships between cell stiffness and cell prestress confirms the validity of this approach [34].

Two-element rheological model:

The two-compartment model basically consists of a series of two viscoelastic solid (Voigt) bodies representing two individualized cytoskeleton components with specific properties. These mechanical properties are defined by best curve fittings of experimental response from the following equation which describes the time course of bead deviation θ(t) during a given stepwise loading:

$$\theta(t)=\frac{\sigma}{E1}\left(1-e^{-\frac{t}{\tau_1}}\right)+\frac{\sigma}{E2}\left(1-e^{-\frac{t}{\tau_2}}\right) \qquad \textbf{(1)}$$

E1 and E2 are the elasticity modulus and τ_1 and τ_2 are the time constants of the cortical and deep cytoskeleton compartments which correspond to respectively a rapidly responsive submembranous "cortical" cytoskeleton associated to the low F-actin density structure and a slowly responsive "deep" cytoskeleton associated to the dense F-actin structure. σ is the mechanical stress applied (equal to the ratio of initial magnetic torque modulus to bead volume) corrected for geometrical effects (notably the angle of bead immersion in the cytoplasm), This model has been previously proposed by our group for its mechanical and biological consistency with experimental data in living cells [18,21]. For instance, the rapidly responsive cortical cytoskeleton compartment appears softer than the deep compartment which is consistent with a larger and faster adaptability of the cortical component to the local environment. On the other hand, the more rigid and slower deep compartment is consistent with the need to maintain cell stability and cell anchorage to substrate.

Results and Discussion

Feasibility of the cellular model (Fig. 2):

First, it should be noted that we were able to measure the mechanical properties of AMs co-cultured, i.e., adherent, over the confluent of monolayer of alveolar epithelial cells because AMs do bind the RGD coated beads (Fig. 1) but the underlying type II alveolar cells could not. This is illustrated by Figure 1 which shows a partial view of the co-culture of macrophages adhering on pneumocytes II. Noteworthy, the spherical beads of 4.5 μm in diameter appear exclusively attached to the AMs just because RGD-coated beads, which came in contact with pneumocytes II, could not adhere and were removed by lavages. Indeed, we have already found that the mechanical characterization by RGD-coated beads of a confluent monolayer of type II alveolar epithelial cells was not possible due to the lack of attached

beads [27], most likely because during these 5-days culture, cells acquire a strong apico-baso-lateral polarity with tight junctions, letting no free integrin on apical side of the confluent monolayer of type II alveolar epithelial cells [9]. This polarity presumably induces a redistribution of integrins receptors towards the basal face, impeding RGD coated beads to attach to the apical face through integrin receptors.

Figure 2A-C shows that the 4.5 µm RGD coated beads are largely embedded in the AM cytoplasm (evidenced by the large bead immersion half angle >100° in AMs illustrated in Fig 2 B and C) and also tightly connected to the F-actin structure. Noteworthy, both the cortical F-actin structure (in grey in Fig. 2) and the deep F-actin structure (in white in Fig. 2), are present and likely attached to the bead. It is interesting to point out, based on the cross-sectional view (Fig 2C), that not only the cortical structure but also the dense F-actin structure are organized around the bead. These 3D-reconstructions demonstrate also that F-actin structure in AMs strongly differ from the actin structure standardly found in adherent cells. These images are also used to prove the effectiveness of the RGD-coated bead attachment to F-actin structure, evidenced by the large bead embedment in the cytoplasm and by the local remodeling of the AM cytoskeleton in response to the bead. This justifies the use of a bead twisting method (MTC) to measure mechanical properties in cells such as alveolar macrophages which are almost not affected by cytochalasin D treatment (see below).

Stiffness specificity of cortical and deep cytoskeleton structures (Fig. 3):

We found that both the cortical and deep cytoskeleton structures exhibit a statistically significant decrease in stiffness when the rigid plastic substrate is replaced by the soft confluent monolayer of type II alveolar epithelial cells (see Figure 3). More precisely, the mean values (+/-SEM) of cortical and deep cytoskeleton elasticity modulus are respectively: E_1=39 Pa ± 3 and E_2 =115 Pa ± 7 for AMs adhering on rigid plastic substrate. These values

are higher than the values obtained for AMs adhering on a confluent monolayer of type II alveolar epithelial cells, namely E_1= 25 Pa ± 3 and E_2 = 86 Pa ± 7. These results clearly show that stiffness of underlying substrate affects the AM stiffness. Note also that substituting epithelial cell monolayer for plastic/glass substrate corresponds to huge drop in elasticity modulus, (i.e., by 7 orders of magnitude). Another important result obtained by MTC is that stiffness of the cortical and the deep cytoskeleton structures of AMs is not affected by cytochalasin D treatment. Indeed, the cortical and deep cytoskeleton stiffness values measured during cytochalasin D treatment are: E_1= 41 Pa ± 4 and E_2= 24 Pa ± 4.2 for glass substrate and E_1= 136 Pa ± 7 and E_2 = 91 Pa ± 12 for cellular substrate which mean no significant difference in terms of cellular stiffness in spite of the blockage of F-actin polymerisation induced by cyto D. Such a result might be surprising if we consider that in tissue cells, the deep cytoskeleton and to a lesser extent the cortical cytoskeleton, was found to be highly sensitive to cyto D treatment. Note however that AMs and alveolar epithelial cells exhibit a common behaviour in terms of range of viscoelastic time constant for the cortical and the deep cytoskeleton, i.e., $\tau_1 = 0.3 – 0.5s \pm 0.03$ while $\tau_2 = 30s \pm 6$.

Influence of biological versus non biological substrates on F-actin structure of AMs (Figs. 4 and 5):

Over a large population of 600-1000 AMs cultured on rigid glass substrate, we have found that the majority of AMs (more than 65%) exhibited a flattened shape. By contrast, the same AMs cultured on a cellular monolayer substrate, exhibited by more of 90% rounded shapes. Confocal cumulative side view of F-actin structures in two adherent AMs with typical symmetrical shape (i.e., without front-rear F-actin polarisation) are presented on the right upper side of Fig. 4A and 4B. On the two graphs of Fig 4A and 4B, we have plotted (on vertical axis) the cumulated surface area of AMs versus the altitude in µm from the bottom

plane (horizontal axis). These graphs reveal that AM shapes are totally dependent on substrate properties. On rigid glass substrates, AMs are flattened with a large cumulated area of more than 600 μm^2 near the basal plane. By contrast, on cellular monolayer substrate, AMs are rounded with a maximum cumulated area of only 200 μm^2 appearing 4-5 µm above the basal plane. Moreover, typical height of macrophages totally differ, namely AMs are 7 µm height on glass substrate but reach 12 µm height on the cellular monolayer substrate.

The views of cortical (in grey) and deep (in white) actin structures in the same AMs are shown after reconstruction in Fig. 5 (oblique views of external: 5A and 5B, external top views: 5C and 5D, and side views of cutting plane: 5E and 5F). Comparing the AM structures on glass (Figs 5A, 5C, 5E) and cellular monolayer (Figs 5B, 5D, 5F) substrates, it can be said that: (i) filipodia/lamilipodia formation generally (the front with intense polymerisation) is essentially planar on rigid substrate but more spatial on cellular substrate (Fig 5A *vs* 5B), (ii) cortical (in grey) and dense F-actin structure (in white) exhibit quite different organisations with a circular structure of dense F-actin at the beginning of the lamellipodia on glass substrate while the dense structure is more homogeneously distributed within the rounded cortical shape on cellular substrate (Figs 5C *vs* 5D), (iii) The cortical structure resembles to a submembranous mantle thinner on glass substrate than on cellular monolayer substrate, with no evidence of stress fibers or F-actin bundles (even in the case of glass substrate) in spite of the evidence of dense actin structures (Figs 5E *vs* 5F). It appears that on cellular substrates, F-actin structure of AMs are closely linked to the F-actin structure of the underlying cellular substrate, suggesting a physical continuity of the connection: F-actin of AMs / integrins / ICAM 1 receptors / F-actin of pneumocytes II at the sites of adherence. Still concerning Fig. 5, it should be said that the boundary between actin structures of AMs (in white and grey) and of pneumocytes II (in violet) is not easily distinguishable and might occur at a cell height of about 1 µm. Note also that F-actin staining in the alveolar epithelial cells forming the

underlying cellular monolayer (in violet in Fig. 5 B, D, F) in only partial (hence the mistaken impression of discontinuity of the cellular monolayer in Fig. 5 B, D, F), while the F-actin staining in AMs is total, providing confident spatial reconstructions of AM structure.

Note that staining of F-actin in alveolar epithelial cells of the monolayer is only partial giving the confusing impression that the cellular monolayer is not confluent (Figs 5 B, D, F). This impression does not correspond to the reality since we verified by different methods (see Material and Methods and the microscopic image in Fig 1) the absolute continuity of the alveolar epithelial cell monolayer.

Note that adhesion sites are not visible on structural images except that punctuated structures of dense actin are visible in the basal plane of AMs (see the basal plane of structures shown in Figs 2C, 4A, 4B, 5E and 5C). In a previous paper [9], we provide some additional evidence that these punctuated structures of actin could be podosomes. Indeed, podosomes which are short-lived punctuate adhesion structures through which AMs adhere, are formed by a diffuse membrane domain of integrins and associated proteins (e.g., vinculin and talin) surrounding a dense actin core [5]. In a recent study, the dynamic nature of these podosomes-like adhesion sites has been characterized from fibroblasts adhering on different matrix rigidities [4]. In the macrophage model presently studied, there is no doubt that these podosomes-like adhesion sites play a key role in the interaction between AMs and substrate (either glass or cellular monolayer). This suggests that the mechanosensitivity of AMs to the substrate properties would most likely be mediated by these specific adhesion sites which actually would act as mechanosensors of the passive mechanical properties of the substrate.

Conclusions

Present results concern the cell sensitivity to substrate stiffness of non activated and mostly non migrant alveolar macrophages. These non tissue cells are for the first time

evaluated structurally and mechanically through two selected components of their cytoskeleton namely the cortical and the deep cytoskeleton components. As previously proposed for alveolar epithelial cells, the cortical cytoskeleton component of AMs evidenced by the lowest F-actin density detectable on confocal images is assumed to be satisfactorily described the rapid and softer viscoelastic compartment while the deep cytoskeleton component evidenced by an intermediate F-actin density is assumed to be satisfactorily described by the slow and stiffer compartment [18]. The two different substrates tested are (i) a non biological rigid plastic/glass substrate routinely used in *in vitro* cellular studies (Young Modulus ~ 3 / 70 MPa respectively) and (ii) a more biological and thus soft cellular substrate made of a confluent monolayer of type II alveolar epithelial cells (Young Modulus ~ 0.1 kPa). Mechanical results were obtained by the Magnetic Twisting Cytometry method earlier described [20,32] and analyzed in terms of stiffness of cortical and deep cytoskeleton components whose mechanical and biological relevance has already been shown for alveolar epithelial cells [18]. Structural results concern the spatial reconstructions of cortical and deep cytoskeleton from confocal images treated at two levels of fluorescence intensity [10]. It is noteworthy that in alveolar macrophages, mechanical results are consistent with structural results and reveal a significant substrate-dependent alveolar macrophage remodelling, which notably depends on the stiffness of the substrate tested. Importantly, this remodeling which reflects the cellular response after three hours of macrophage culture on either rigid or soft substrates, implicates the whole cytoskeleton. Note however that the deep component of macrophages does not resemble to the deep component of alveolar epithelial cells. Indeed, in macrophages, the deep cytoskeleton does not exhibit stress fibers whereas its sensitivity to cytochalasin D treatment is negligible. The same lack of sensitivity to cytochalasin D is observed for the cortical cytoskeleton component of alveolar macrophages. These results mean that both the cortical and the deep cytoskeleton have a negligible internal tension,

consistently with the lack of stress fibers. Hence the need to consider pathways for the mechanosensivity of alveolar macrophage which could differ from the pathways classically proposed to describe mechanotransduction in tensed tissue cells, (i.e., focal contacts, integrins, tensed actin stress fibers transmitting eventually distant acto-myosin contraction) [2,13,17,36]. Based on present results, we have recently proposed [9] that non actinic cytoskeleton filament such as microtubules - which have been shown to be in direct contact with podosomes [22] - coupled with the contractile apparatus present at the level of podosomes [30] could act as mechanosensitive pathways specific to alveolar macrophages. Importantly, it has been shown that force regulation through highly dynamic adhesion sites to which podosomes pertain, could be controlled by substrate mechanical properties [1,4]. In other words, the immature (i.e., nascent) character of adhesion sites seems to be required to match the exerted forces to the stiffness of the substrate [3,26]. Hence, due to their dynamic adhesion sites (podosomes), alveolar macrophages could sense mechanical properties of their environment. Interestingly enough, present results indicate that biologically relevant substrate (here a cellular monolayer) might enhance the sensitivity of alveolar macrophages to their spatial environment which can be suggested by the generation of 3D filopodic extensions shown in Figs 5B.

From a cellular engineering point of view, the present study is a new demonstration that there is a need to perform *in vitro* cellular studies using realistic substrate conditions which notably means the control of mechanical properties of extracellular matrix. We are aware that in the present study, adhesion conditions were certainly different between the glass/plastic substrate and the cellular substrate which could in turns contribute for a part to the measured stiffness. Incidentally, the expected higher affinity of alveolar macrophages for the cellular substrate does not necessarily result in higher cellular stiffness but, on the contrary in lower stiffness.

To conclude, the present study can be seen as a new contribution to the rapidly growing field of mechanobiology in which mechanical properties of the cellular environment contribute, in relation with the cytoskeleton, to the overall cell response.

Acknowledgments

Authors gratefully thank Région d'Ile-de-France for financial support of the AFM equipment acquired by University Paris XII.

Legend of Figures

Figure 1: Light microscopy image of two alveolar macrophages (AMs) adherent on a confluent monolayer of type II alveolar epithelial cells (AECs) (objective ×20). Each macrophage is surmounted by an RGD-coated ferromagnetic bead (Ø = 4.5 µm) partially immersed in the cytoplasm of macrophages. Note that RGD-coated beads could not adhere on type II alveolar epithelial cells (AECs). Indeed, due to their strong apico-baso-lateral polarity, these cells do not express integrins on their apical face and RGD coated beads could not adhere. By contrast alveolar macrophages adhere on AECs because their integrins are linked to the Inter Cellular Adhesion Molecules expressed by AECs on the apical face. AECs exhibit secretary vesicules (SV) visible on their upper face which should not be confounded with the beads used for probing cell mechanical properties.

Figure 2: 3D reconstructions of cortical and deep actin cytoskeleton structure in a given alveolar macrophages (in A: viewed from top, in B: viewed from side, in C: cross-sectional view). These reconstructions were obtained from Z-stack images obtained by confocal

microscopy after staining F-actin with rhodamined phalloidin. Spatial contours of cortical (external) and deep (internal) F-actin structures were obtained for minimal and intermediate levels of fluorescence intensity (see text for explanation). The cutting plane view shown in C is performed according to the axis (shown in A) which crosses the ferromagnetic bead. B and C show that the bead is largely immersed in the cytoplasm (half-angle of bead immersion around 100°) and in close relationships with cortical and deep F-actin structures. Each square is 10 μm in all images.

Figure 3:

Cortical (in A) and deep (in B) "cytoskeleton elasticity modulus", also called in the text "cortical and/or deep stiffness" and noted E_1 and E_2 respectively, measured in alveolar macrophages adhering on rigid plastic substrate (left columns) or on a soft confluent monolayer of type II alveolar epithelial cells (right columns). Measurements were made by Magnetic Twisting Cytometry and were analyzed by a model made of two viscoelastic solid (Voigt) element in series representing two individualized cytoskeleton components with specific properties. In full dark: control values; In grey: after 11 min of F-actin depolymerizing treatment with cytochalasin D. Values are mean ± s.e.m. Each value is the mean of three independent measurements. The statistical test used here is the Anova test. There is a significant decrease in both cortical and deep cytoskeleton elasticity modulus ($n = 19$ for control values, $n = 7$ (on plastic) and 12 (on cell substrate) for cytochalasin D treatment). Values of cortical and deep elasticity modulus in alveolar macrophages are not affected by cytochalasin D treatment (see Results).

Figure 4:

Characterization of typical AM shapes obtained for the two different substrates namely the rigid glass substrate (in A) and the confluent monolayer of type II alveolar epithelial cells (in B). Graphs represent the cumulated spreading area (in μm^2) of alveolar macrophages versus the cell height in µm. These geometrical values are calculated from the optical planes obtained by confocal microscopy. The corresponding spatial visualizations are shown on the right upper corner of each graph and represent the entire cumulated fluorescent intensity (intensity increases from orange to yellow). The length scale is 10 µm.

Figure 5:

3D reconstructions of the cortical (in grey) and deep (in white) actin cytoskeleton structure in alveolar macrophages adherent on rigid glass substrate (images on left column: A, C, E) or on confluent monolayer of type II alveolar epithelial cells (images on right column: B, D, F). Oblique views (in A and B), top view (in C and D), cutting plane views (in E and F) following the vertical plane defined by the dotted line shown in C and D. Note that the cortical (lowest detectable F-actin density) and the deep (intermediate F-actin density) actin cytoskeleton components clearly differ in terms of structures, depending on the type of substrate used. Note also that F-actin staining in the type II alveolar epithelial cells (in violet) forming the underlying confluent monolayer in only partial (hence the mistaken impression of discontinuity of the cellular monolayer), while the F-actin staining in AMs is total. These 3D-reconstruction views were obtained from Z-stack images issued from confocal microscopy with ×100 objective. Each square is 10 µm.

References

[1] R. F. Bruinsma. Theory of Force Regulation by Nascent Adhesion Sites, *Biophysical Journal* **89** (2005), 87-94.

[2] M. Chiquet, A. S. Renedo, F. Huber and M. Fluck. How do fibroblasts translate mechanical signals into changes in extracellular matrix production?, *Matrix Biol* **22** (2003), 73-80.

[3] D. Choquet, D. P. Felsenfeld and M. P. Sheetz. Extracellular Matrix Rigidity Causes Strengthening of Integrin-Cytoskeleton Linkages, *Cell* **88** (1997), 39-48.

[4] O. Collin, P. Tracqui, A. Stephanou, Y. Usson, J. Clement-Lacroix and E. Planus. Spatiotemporal dynamics of actin-rich adhesion microdomains: influence of substrate flexibility, *Journal Of Cell Science* **119** (2006), 1914-1925.

[5] O. Destaing, F. Saltel, J. C. Geminard, P. Jurdic and F. Bard. Podosomes display actin turnover and dynamic self-organization in osteoclasts expressing actin-green fluorescent protein, *Mol Biol Cell* **14** (2003), 407-416.

[6] D. E. Discher, P. Janmey and Y. L. Wang. Tissue cells feel and respond to the stiffness of their substrate, *Science* **310** (2005), 1139-1143.

[7] B. Doornaert, V. Leblond, E. Planus, S. Galiacy, V. M. Laurent, G. Gras, D. Isabey and C. Lafuma. Time course of actin cytoskeleton stiffness and matrix adhesion molecules in human bronchial epithelial cell cultures, *Exp Cell Res* **287** (2003), 199-208.

[8] A. J. Engler, M. A. Griffin, S. Sen, C. G. Bonnemann, H. L. Sweeney and D. E. Discher. Myotubes differentiate optimally on substrates with tissue-like stiffness: pathological implications for soft or stiff microenvironments, *J Cell Biol* **166** (2004), 877-887.

[9] S. Féréol, R. Fodil, B. Labat, S. Galiacy, V. M. Laurent, B. Louis, D. Isabey and E. Planus. Sensitivity of alveolar macrophages to substrate mechanical and adhesive properties, *Cell Motil Cytoskeleton* **63** (2006), 321-340.

[10] R. Fodil, V. M. Laurent, E. Planus and D. Isabey. Characterization of cytoskeleton mechanical properties and 3D-actin structure in twisted living adherent cells, *Biorheology* **40** (2003), 241-245.

[11] G. Forgacs. On the possible role of cytoskeletal filamentous networks in intracellular signaling: an approach based on percolation., *Journal Of Cell Science* **108** (1995), 2131-2143.

[12] Y.-C. Fung. *Biomechanics: mechanical properties of living tissues.*, Springer-Verlag, New York, 1993.

[13] C. G. Galbraith and M. P. Sheetz. Forces on adhesive contacts affect cell function, *Current opinion in cell biology* **10** (1998), 566-571.

[14] A. Gefen and S. S. Margulies. Are in vivo and in situ brain tissues mechanically similar?, *J Biomech* **37** (2004), 1339-1352.

[15] P. C. Georges and P. A. Janmey. Cell type-specific response to growth on soft materials, *J Appl Physiol* **98** (2005), 1547-1553.

[16] F. M. Hendriks, D. Brokken, C. W. Oomens, D. L. Bader and F. P. Baaijens. The relative contributions of different skin layers to the mechanical behavior of human skin in vivo using suction experiments, *Med Eng Phys* **28** (2006), 259-266.

[17] D. Ingber. Integrins as mechanochemical transducers, *Current opinion in cell biology* (1991), 841-848.

[18] V. M. Laurent, R. Fodil, P. Canadas, S. Fereol, B. Louis, E. Planus and D. Isabey. Partitioning of cortical and deep cytoskeleton responses from transient magnetic bead twisting, *Ann Biomed Eng* **31** (2003), 1263-1278.

[19] V. M. Laurent, R. Fodil, P. Cañadas, E. Planus and D. Isabey. Specific Mechanical and Structural Responses of Cortical and Cytosolic Cytoskeleton in Living Adherent Cells, *JSME International Journal (Series C)* **45** (2002), 897-905.

[20] V. M. Laurent, S. Henon, E. Planus, R. Fodil, M. Balland, D. Isabey and F. Gallet. Assessment of mechanical properties of adherent living cells by bead micromanipulation: comparison of magnetic twisting cytometry vs optical tweezers, *Journal of Biomechanical Engineering* **124** (2002), 408-421.

[21] V. M. Laurent, E. Planus, R. Fodil and D. Isabey. Mechanical assessment by magnetocytometry of the cytosolic and cortical cytoskeletal compartments in adherent epithelial cells, *Biorheology* **40** (2003), 235-240.

[22] S. Linder, K. Hufner, U. Wintergerst and M. Aepfelbacher. Microtubule-dependent formation of podosomal adhesion structures in primary human macrophages, *Journal Of Cell Science* **113 Pt 23** (2000), 4165-4176.

[23] C. M. Lo, H. B. Wang, M. Dembo and Y. L. Wang. Cell movement is guided by the rigidity of the substrate, *Biophys J* **79** (2000), 144-152.

[24] J. Ohayon, P. Tracqui, R. Fodil, S. Féréol, V. M. Laurent, E. Planus and D. Isabey. Analysis of nonlinear responses of adherent epithelial cells probed by magnetic bead twisting: a finite element model based on a homogenization approach, *Journal Biomechanical Engineering (ASME)* **126** (2004), 685-698.

[25] M. J. Paszek, N. Zahir, K. R. Johnson, J. N. Lakins, G. I. Rozenberg, A. Gefen, C. A. Reinhart-King, S. S. Margulies, M. Dembo, D. Boettiger, D. A. Hammer and V. M. Weaver. Tensional homeostasis and the malignant phenotype, *Cancer Cell* **8** (2005), 241-254.

[26] R. J. Pelham, Jr. and Y. Wang. Cell locomotion and focal adhesions are regulated by substrate flexibility, *Proc Natl Acad Sci U S A* **94** (1997), 13661-13665.

[27] E. Planus, S. Galiacy, M. Matthay, V. Laurent, J. Gavrilovic, G. Murphy, C. Clérici, D. Isabey, C. Lafuma and M. P. d'Ortho. Role of collagenase in mediating in vitro alveolar epithelial wound repair, *Journal Of Cell Science* **112 (Pt 2)** (1999), 243-252.

[28] J. Pourati, A. Maniotis, D. Spiegel, J. L. Schaffer, J. P. Butler, J. J. Fredberg, D. E. Ingber, D. Stamenovic and N. Wang. Is cytoskeletal tension a major determinant of cell deformability in adherent endothelial cells?, *American Journal of Physiology* **274** (1998), C1283-1289.

[29] M. D. Rossman, A. M. Cassizzi and R. P. Daniele. Adherence and morphology of guinea pig alveolar macrophages: effect of N-formyl methionyl peptides, *Infect Immun* **29** (1980), 1185-1189.

[30] J. Tanaka, T. Watanabe, N. Nakamura and K. Sobue. Morphological and biochemical analyses of contractile proteins (actin, myosin, caldesmon and tropomyosin) in normal and transformed cells, *Journal Of Cell Science* **104 (Pt 2)** (1993), 595-606.

[31] H. B. Wang, M. Dembo, S. K. Hanks and Y. Wang. Focal adhesion kinase is involved in mechanosensing during fibroblast migration, *Proc Natl Acad Sci U S A* **98** (2001), 11295-11300.

[32] N. Wang, J. P. Butler and D. E. Ingber. Mechanotransduction across the cell surface and through the cytoskeleton [see comments], *Science* **260** (1993), 1124-1127.

[33] N. Wang and Z. Suo. Long-distance propagation of forces in a cell, *Biochem Biophys Res Commun* **328** (2005), 1133-1138.

[34] N. Wang, I. M. Tolic-Norrelykke, J. Chen, S. M. Mijailovich, J. P. Butler, J. J. Fredberg and D. Stamenovic. Cell prestress. I. Stiffness and prestress are closely associated in adherent contractile cells, *Am J Physiol Cell Physiol* **282** (2002), C606-616.

[35] S. Wendling, E. Planus, V. Laurent, L. Barbe, A. Mary, C. Oddou and D. Isabey. Role of cellular tone and microenvironmental conditions on cytoskeleton stiffness assessed by tensegrity model, *European Physical Journal Applied Physics* **9** (2000), 51-62.

[36] K. M. Yamada. Integrin signaling, *Matrix Biology* **16** (1997), 137-141.

[37] T. Yeung, P. C. Georges, L. A. Flanagan, B. Marg, M. Ortiz, M. Funaki, N. Zahir, W. Ming, V. Weaver and P. A. Janmey. Effects of substrate stiffness on cell morphology, cytoskeletal structure, and adhesion, *Cell Motil Cytoskeleton* **60** (2005), 24-34.

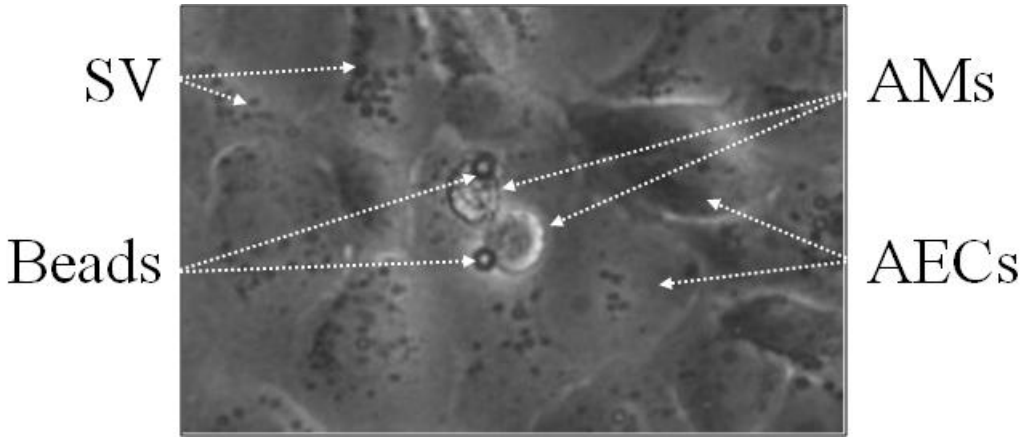

Figure 1

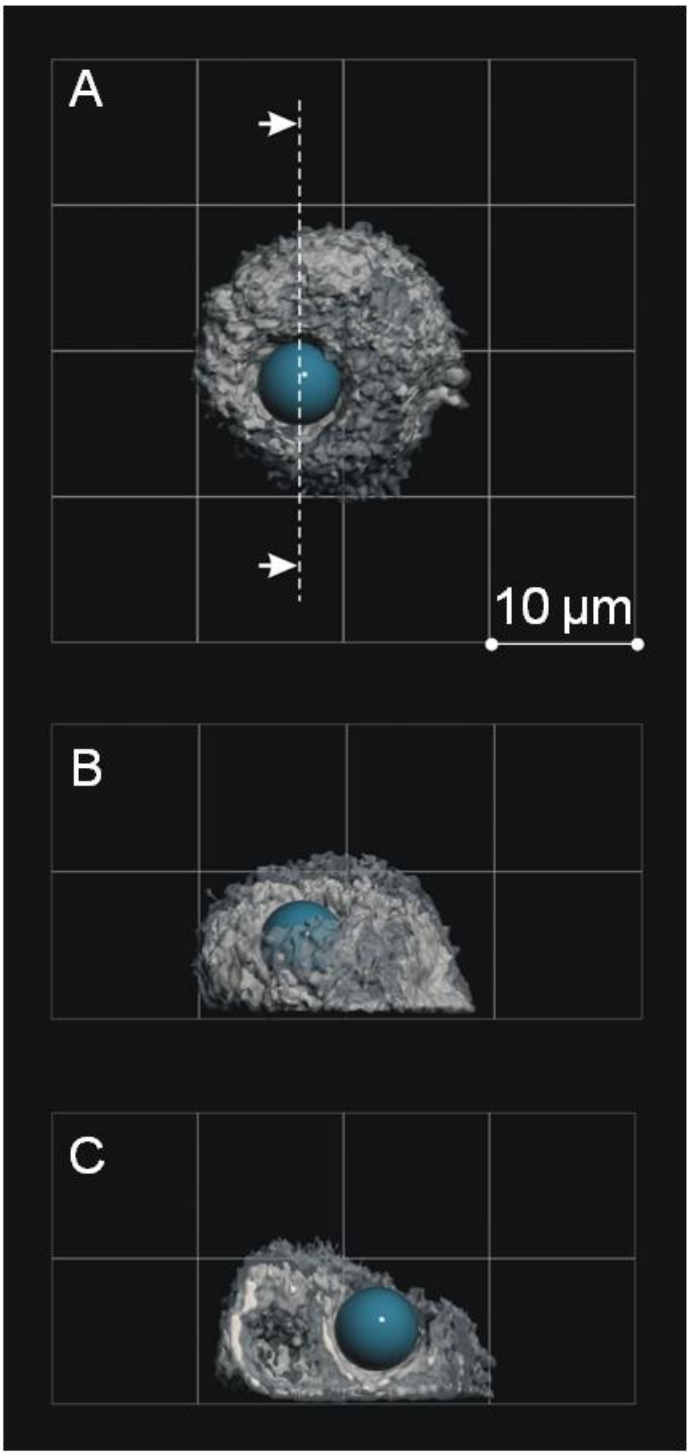

Figure 2

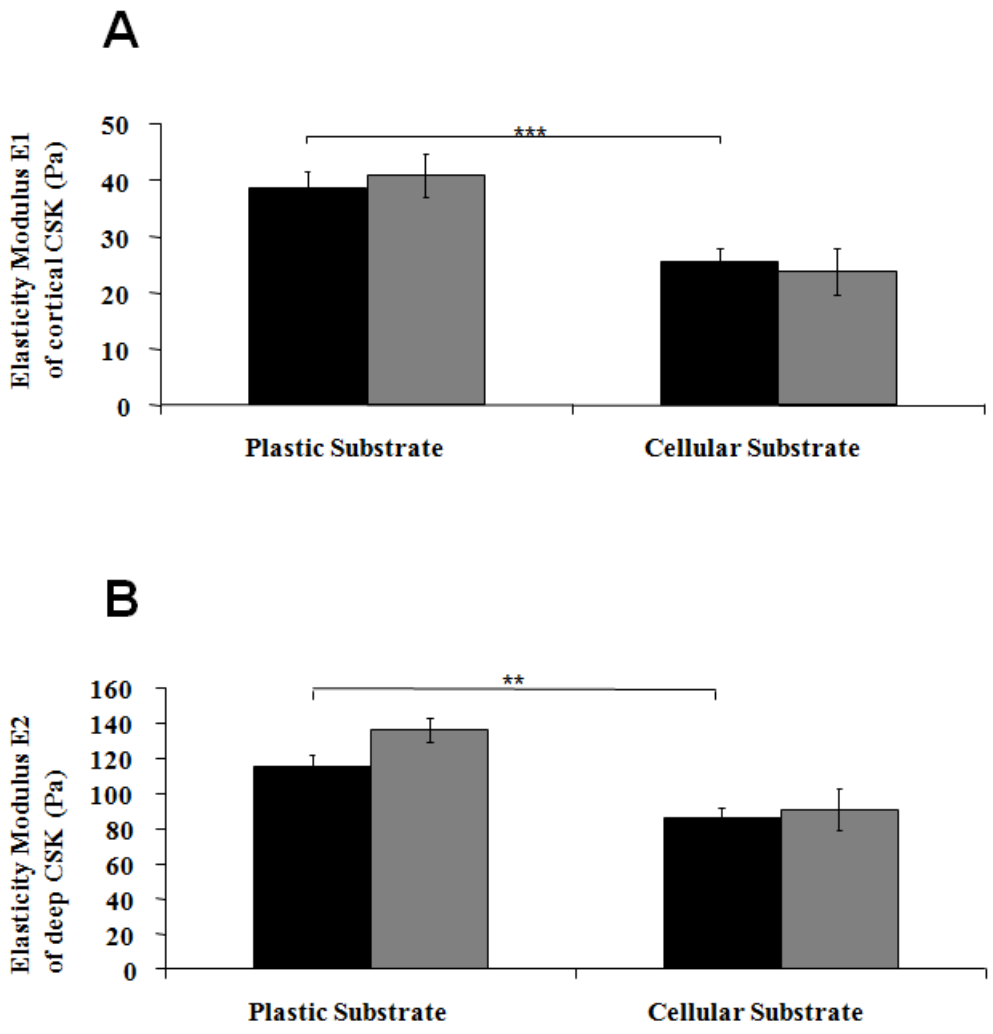
A
Elasticity Modulus E1
of cortical CSK (Pa)
50
40
30
20
10
0
***
Plastic Substrate
Cellular Substrate
B
Elasticity Modulus E2
of deep CSK (Pa)
160
140
120
100
80
60
40
20
0
**
Plastic Substrate
Cellular Substrate

Figure 3

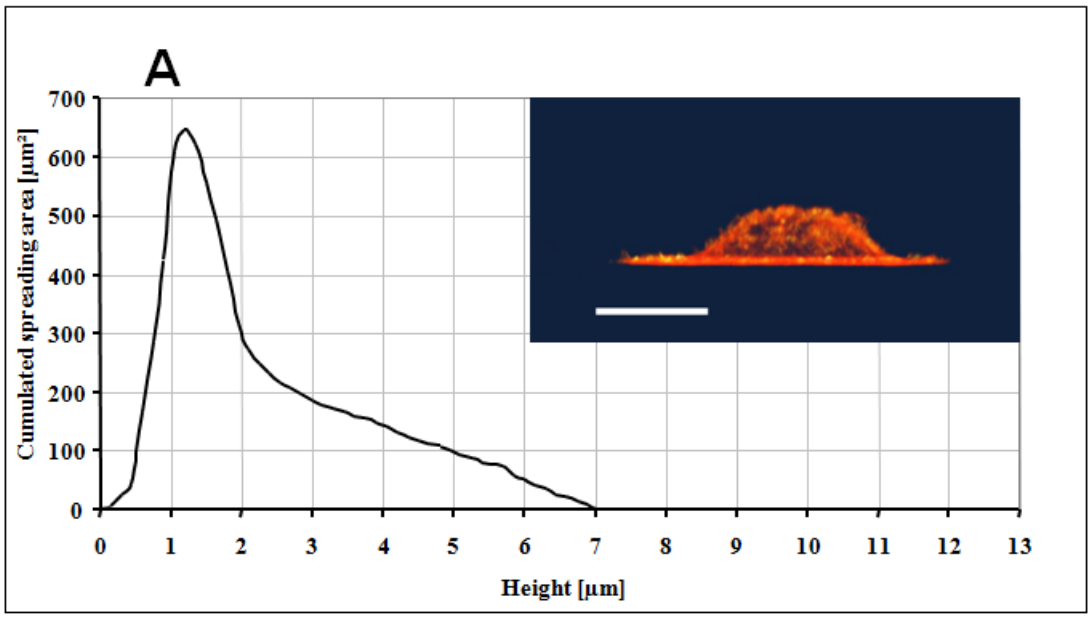
A
Cumulated spreading area [µm²]
700
600
500
400
300
200
100
0
0 1 2 3 4 5 6 7 8 9 10 11 12 13
Height [µm]

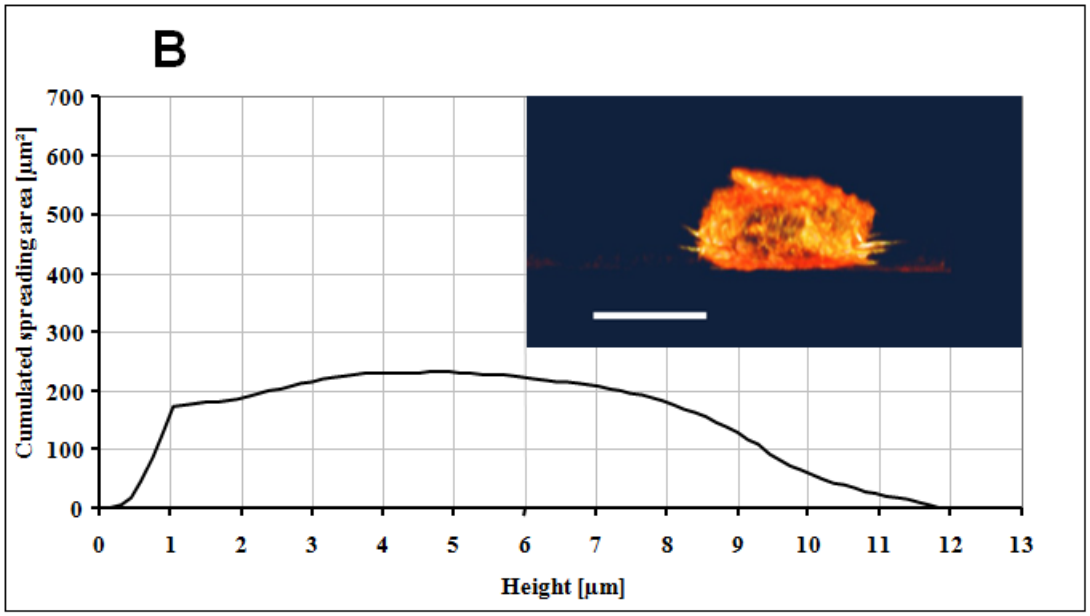
B
Cumulated spreading area [µm²]
700
600
500
400
300
200
100
0
0 1 2 3 4 5 6 7 8 9 10 11 12 13
Height [µm]

Figure 4

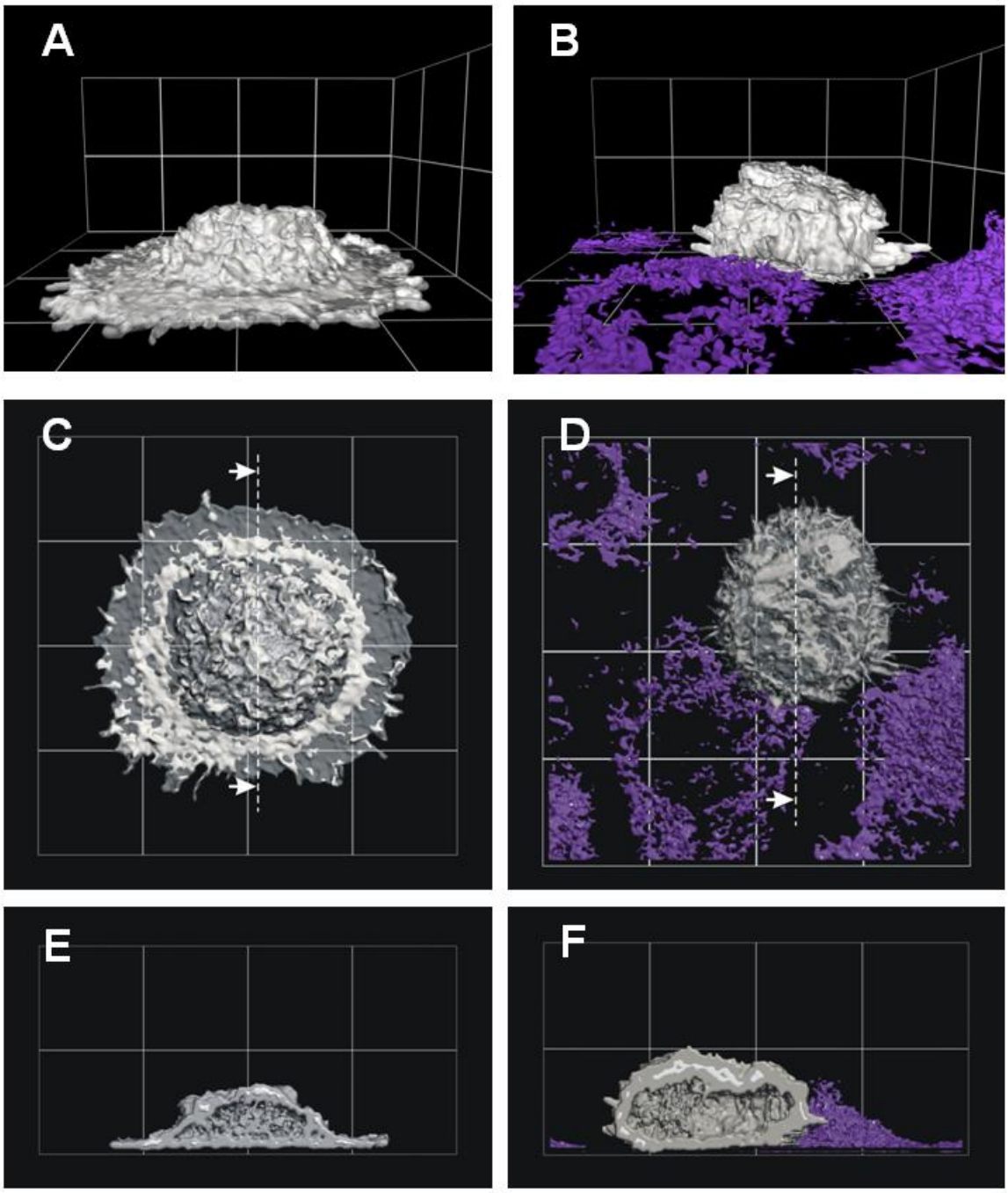

Figure 5